Title
Automated Detection, Localization, and Classification of Traumatic Vertebral Body Fractures in the Thoracic and Lumbar Spine at CT.

Journal
Radiology, 278(1)

ISSN
0033-8419

Authors
Burns, Joseph E
Yao, Jianhua
Muñoz, Hector
et al.

Publication Date
2016

DOI
10.1148/radiol.2015142346

Peer reviewed

Radiology

Automated Detection, Localization, and Classification of Traumatic Vertebral Body Fractures in the Thoracic and Lumbar Spine at CT[1]

Joseph E. Burns, MD, PhD
Jianhua Yao, PhD
Hector Muñoz, BS
Ronald M. Summers, MD, PhD

Purpose: To design and validate a fully automated computer system for the detection and anatomic localization of traumatic thoracic and lumbar vertebral body fractures at computed tomography (CT).

Materials and Methods: This retrospective study was HIPAA compliant. Institutional review board approval was obtained, and informed consent was waived. CT examinations in 104 patients (mean age, 34.4 years; range, 14–88 years; 32 women, 72 men), consisting of 94 examinations with positive findings for fractures (59 with vertebral body fractures) and 10 control examinations (without vertebral fractures), were performed. There were 141 thoracic and lumbar vertebral body fractures in the case set. The locations of fractures were marked and classified by a radiologist according to Denis column involvement. The CT data set was divided into training and testing subsets (37 and 67 subsets, respectively) for analysis by means of prototype software for fully automated spinal segmentation and fracture detection. Free-response receiver operating characteristic analysis was performed.

Results: Training set sensitivity for detection and localization of fractures within each vertebra was 0.82 (28 of 34 findings; 95% confidence interval [CI]: 0.68, 0.90), with a false-positive rate of 2.5 findings per patient. The sensitivity for fracture localization to the correct vertebra was 0.88 (23 of 26 findings; 95% CI: 0.72, 0.96), with a false-positive rate of 1.3. Testing set sensitivity for the detection and localization of fractures within each vertebra was 0.81 (87 of 107 findings; 95% CI: 0.75, 0.87), with a false-positive rate of 2.7. The sensitivity for fracture localization to the correct vertebra was 0.92 (55 of 60 findings; 95% CI: 0.79, 0.94), with a false-positive rate of 1.6. The most common cause of false-positive findings was nutrient foramina (106 of 272 findings [39%]).

Conclusion: The fully automated computer system detects and anatomically localizes vertebral body fractures in the thoracic and lumbar spine on CT images with a high sensitivity and a low false-positive rate.

Online supplemental material is available for this article.

[1] From the Department of Radiological Sciences, University of California–Irvine, Orange, Calif (J.E.B.); and Imaging Biomarkers and Computer-Aided Detection Laboratory, Radiology and Imaging Sciences, National Institutes of Health Clinical Center, 10 Center Dr, Building 10, 1C224, MSC1182, Bethesda, MD 20892-1182 (J.Y., H.M., R.M.S.).
Received October 15, 2014; revision requested December 16; revision received April 4, 2015; accepted April 16; final version accepted May 14.
Address correspondence to R.M.S. (e-mail: *rms@nih.gov*).

Traumatic spine injuries are common, with an estimated 140 000–160 000 vertebral fractures per year in the United States. An estimated 19%–50% of thoracic and lumbar spine fractures are associated with neurologic deficits (1,2). Rapid diagnoses with accurate and detailed characterization of the injury are increasingly important to guide patient treatment decisions (3,4). Efforts by the trauma surgery community to create standards for patient care and improve treatment outcomes have resulted in the development of a number of spine injury classification systems (5–12). These classification systems are based on detailed morphologic data from patients' imaging studies; they affect treatment decisions for intervention versus conservative treatment and guide decision making for surgical approach and optimal fixation interval (4,13–15). Classification of spine fracture patterns into these sometimes complex schemes can be a time-consuming task, resulting in additional work for the radiologist in this era of commensurately increasing workloads and study complexity (16,17). An example of a complex injury classification schema is the Magerl-AO (Arbeitsgemeinschaft für Osteosynthesefragen) system, with 53 potential categories for assignment of the detected vertebral fracture pattern (18).

No universally accepted classification system has been devised to date, and classification protocols continue to develop. Although varying in detail, these systems typically allow classification of fractures on the basis of spinal stability considerations, with focus on the main load-bearing component, the vertebral body (19).

Prior work in the assessment of vertebral bodies for anterior height loss to detect fractures on lateral radiographs, oriented toward osteoporotic compression fractures, has reached clinical application (20,21). Additionally, research has been conducted for computerized assessment of compression fractures through the detection of vertebral body height loss on midline sagittal sections of lumbar computed tomographic (CT) images and on three-dimensional volumetric renderings (22,23). However, simple height measurement is not sufficient for fracture categorization in a number of spine trauma injury classification systems in clinical use. Relatedly, computational assessment of known spine fractures has been performed for preoperative planning, inferring vertebral height loss, canal narrowing, and shear injury by determining the central axis of each vertebral body and anterior-posterior canal diameter (24). Segmentation and analysis of the complex three-dimensional structure of the spine on CT images, with direct quantitative assessment of bone discontinuities that constitute osseous fracture lines, is a novel topic of clinical importance for spine injury diagnosis and classification and is the focus of this article.

Previously, we devised a decision support system for fracture detection on CT images (25). In that initial step, the system was designed to detect fracture lines on the vertebral body cortex. The system presented here has since been extended to generate quantitative fracture metrics, including the location and extent of the fracture, that serve as constituents for fracture classification. As a sample classification task of clinical interest, the system was designed for Denis column fracture involvement of the affected vertebral bodies (7).

The purpose of our study was to design and validate a fully automated computer system for the detection and anatomic localization of vertebral body fractures of the thoracic and lumbar spine through quantitative analysis of CT images.

Advances in Knowledge

- A fully automated computer system has been developed for the detection and anatomic localization of vertebral body fractures of the thoracic and lumbar spine on CT images.
- Our fully automated system demonstrates 92% sensitivity for fracture detection and localization of the correct vertebra, with a false-positive occurrence rate of 1.6 per patient.

Implications for Patient Care

- Although not yet at the point of clinical application, our computer system automatically detects vertebral body fractures in the thoracic and lumbar spine as an initial step toward a fracture detection system that will assess both the vertebral body and posterior elements.
- Our system detects the level of the fractured vertebra and the precise location of the fracture within the vertebra and may assist the radiologist in fracture classification according to orthopedic trauma surgery classification systems.
- The system has the potential to decrease interobserver variability in fracture detection and help standardize fracture reporting.

Materials and Methods

Study Subjects

Our study received institutional review board approval and was compliant with

Published online before print
10.1148/radiol.2015142346 **Content codes:** CT MK

Radiology 2016; 278:64–73

Abbreviations:
CI = confidence interval
FP = false-positive
FPR = FP rate
FROC = free-response receiver operating characteristic
SVM = support vector machine
TP = true-positive

Author contributions:
Guarantor of integrity of entire study, J.E.B.; study concepts/study design or data acquisition or data analysis/interpretation, all authors; manuscript drafting or manuscript revision for important intellectual content, all authors; approval of final version of submitted manuscript, all authors; agrees to ensure any questions related to the work are appropriately resolved, all authors; literature research, J.E.B., J.Y., H.M.; clinical studies, J.E.B.; experimental studies, J.E.B., J.Y., R.M.S.; statistical analysis, J.E.B., J.Y.; and manuscript editing, J.E.B., J.Y., R.M.S.

Funding:
This research was supported by the National Institutes of Health (grants 1Z01 CL040004 and ZIE CL090017-04).

Conflicts of interest are listed at the end of this article.

the Health Insurance Portability and Accountability Act. Since our study was performed as a retrospective analysis of previously obtained imaging studies, informed consent was waived.

The radiology information system application "Radiology Report Search" (RadNet, Cerner Millennium, North Kansas City, Mo) was used to conduct a review of a medical imaging database at a level 1 trauma center for potential spine fracture cases. Radiology information system parameters specified the date of service range for the search, the imaging modality as "computed tomography," and free-text search keywords of "CT+spine+fracture +contrast+(thoracic lumbar)" in the dictated reports. A total of 3528 reports were returned from this search. A Standards for Reporting of Diagnostic Accuracy chart of the methods used is provided in Figure 1.

One author (J.E.B.), a fellowship-trained board-certified musculoskeletal radiologist with 7 years of experience, reviewed filtered reports returned from the radiology information system search. Examinations dictated as being positive for acute fractures of the thoracic or lumbar vertebrae were set aside for picture archiving and communication system, or PACS, review. These cases were reviewed on an AGFA Impax PACS system (AGFA, Mortsel, Belgium), with exclusion criteria for case selection applied during the PACS evaluation. The study set was composed of 94 consecutive nonexcluded examinations that demonstrated one or more vertebral fractures (major spinal injuries) for use as the case set and 10 examinations without vertebral fractures as the control set (7). Of the 94 patients with fractures, 59 patients had one or more vertebral body fractures, including 41 patients with one vertebral body fracture, 11 patients with two vertebral body fractures, five patients with three vertebral body fractures, and two patients with four vertebral body fractures, for a total of 86 vertebral body fractures of the thoracic and lumbar spine in the case set. Thirty-five patients had isolated fractures of posterior elements. The mean age of the patients was 34.4 years with a range of 14–88 years, consisting of 32 female patients and 72 male patients. The mean age of female patients was 43 years (range, 17–88 years), and the mean age of the male patients was 39 years (range, 14–84 years). There was no significant difference in age between men and women (P = .39 with the t test). The dates of performance of the examinations selected ranged from 2009 to 2011.

Image Acquisition

A total of 101 patients selected for the study were scanned with spine CT protocols, and three patients were scanned with body CT protocols. Section thickness and in-plane resolution parameters are included in Table 1. Ninety-five of the 104 patients incidentally received intravenous contrast material as part of their examination protocol.

Lesion Identification

Digital Imaging and Communications in Medicine images for each CT examination were downloaded in a noncompressed

Figure 1

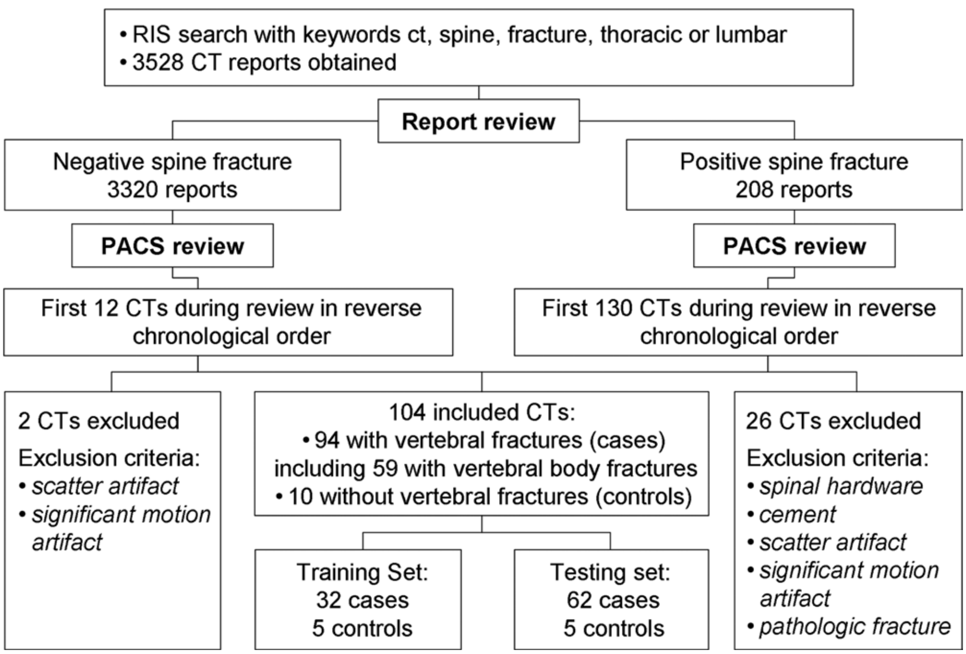

Figure 1: Standards for Reporting of Diagnostic Accuracy chart illustrates case accumulation, exclusion, and partitioning. *PACS* = picture archiving and communication system, *RIS* = radiology information system.

Table 1

Image Acquisition Data

Protocol	Section Thickness* 1 mm	2 mm	5 mm	In-plane Resolution (mm/pixel)	Mean Dose-Length Product (mGy · cm)	Mean Collimation (mm)
Spine				0.26–0.44		
Combined thoracic and lumbar spine	2	86	…		1548.7 (924.0–3631.6)	0.61 (0.6–1.2)
Thoracic spine	1	4	…		1630.0 (727.0–3876.0)	0.64 (0.6–0.8)
Lumbar spine	1	7	…		1187.9 (824.0–1612.0)	0.67 (0.6–1.2)
Body				0.56–0.87		
Chest, abdomen, and pelvis	…	1	…		1552.0	0.6
Abdomen and pelvis	…	1	1		1209.5 (1092.0–1327.0)	0.9 (0.6–1.2)

Note.—The CT scanner used was the Siemens Sensation 64, Erlangen, Germany. Numbers in parentheses are ranges.

* Data are the number of patients with the specified section thickness.

format. One author (J.E.B.) reviewed the images and manually marked the approximate centroid of each fracture locus (defined here as a localized grouping of fracture lines detected as contiguous) on the images. A total of 141 thoracic and lumbar vertebral body fractures were marked. Denis column classification of vertebral body fractures as anterior column, middle column, or both columns was performed. Here, we define the anterior column as the anterior two-thirds of the vertebral body (as seen on a sagittal midline image or axial image) and the middle column as the posterior one-third of the vertebral body (Fig 2) (5,26,27). The CT examinations were then partitioned into training and testing sets. The manually annotated fractures were used as the reference standard.

Figure 2

Figure 2: Axial CT section of the spine in a 28-year-old man with an L1 vertebral body fracture has the anterior and middle Denis columns projected onto it.

Quantitative Image Analysis Methods

A simplified illustration of the methods is provided in Figure E1 and Appendix E1 (online). Spine segmentation was performed with vertebral body partitioning (28). Fracture detection in this preliminary work is limited to the vertebral body to simplify the topological analysis and to focus on structurally important Denis anterior and middle column injuries. A software algorithm was designed for fracture line detection on the vertebral body cortex (25). This algorithm separates the cortex from the medullary space by using deformable dual-surface models to detect, fit, and extract the interior (endosteal) and exterior (periosteal) surfaces, forming a "cortical shell." This shell is mapped into a two-dimensional plane and fracture lines detected with pattern recognition techniques in which multiscale adaptive filtering is used. Fracture detections are then re-embedded into three-dimensional space, and three-dimensional quantitative fracture features are computed.

A committee of support vector machines (SVMs) was used as the system classifier to categorize detections as positive (fracture) or negative (no fracture) and then compare this

SVM categorization with the reference standard data to determine whether there is a true-positive (TP) or false-positive (FP) result (29–33). Training of the SVM committee was performed by using quantitative features extracted from detections in the training case data set of CT studies. This training was based on classifier correlation of automated detection candidates obtained from computer system analysis of the training data set with the reference standard data set of fractures manually marked by an expert radiologist on the same training set.

Ten-fold cross-validation of the classifier system was performed by using the training data with free-response receiver operating characteristic (FROC) analysis, resulting in a trained SVM committee. The final set of computer system detections was obtained by means of analysis of the testing case set by the trained SVM committee classifier. The per-case analysis time for the system was less than 2 minutes on a high-end office desktop computer (Dell Precision T7600 with dual 2.30-GHz central processing unit, 16.0-GB memory, and 64-bit Windows 7 operating system; Dell, Round Rock, Tex).

The origins of false-negative findings (fracture misses) and FP fracture line detections were decided in a consensus review by two board-certified fellowship-trained radiologists (J.E.B. and R.M.S., a fellowship-trained board-certified body imaging radiologist with 19 years of experience). Fracture line detections obtained from quantitative imaging system analysis of the studies that were initially marked as FP by the system but that were subsequently found to be TP lesions that had not been marked in the reference standard set were excluded from the FP statistical analysis.

Table 2

Reference Standard Data Set with Subgroup Data Breakdown

Data Set	No. of Patients	No. of Fracture Loci			No. of Fractured Vertebrae		
		Thoracic	Lumbar	All	Thoracic	Lumbar	All
Training set	37	20	14	34	16	10	26
Testing set	67	54	53	107	31	29	60
All	104	74	67	141	47	39	86

Table 3

Detection Statistics

Data Set	No. of Patients	TP Loci	FP Loci	TP Vertebrae	FP Vertebrae
Training set	37	28 of 34 (82.3)	91	23 of 26 (88.5)	48
Testing set	67	87 of 107 (81.3)	181	55 of 60 (91.7)	106

Note.—Numbers in parentheses are percentages.

Statistical Analysis

FROC curve analysis of the computer system data set classifications was used for assessment of system performance. The FROC curve was generated by varying a threshold on SVM probability (signed distance to the SVM hyperplane) to determine whether a detected finding is a fracture or a nonfracture. A thousand bootstrap replications were performed to obtain the confidence intervals by using bootstrap percentile intervals based on resampling. Bootstrap resampling was conducted at the patient level to take into account the clustering of lesions.

The operating point value in the FROC analysis was chosen to target a sensitivity for computer-aided fracture detection in the training set of 80% or higher, balancing this with the maintenance of a clinically reasonable false-positive rate (FPR). The testing set sensitivity was then calculated by using the same operating point (0.52 in SVM value). A bivariate χ^2 test was used for analysis of the statistical significance of sensitivity value differences between the testing and training sets. For all analyses, a P value less than .05 was considered to indicate a statistically significant difference.

Results

The locations of a total of 141 reference standard fracture loci were marked electronically by a radiologist (J.E.B.) in the patient study set of 104 cases, for a per-patient mean ± standard deviation of 1.4 vertebral body fracture loci ± 1.8 and a range of 0–4 vertebral body fractures per patient. The patient study set was divided into independent training (37 studies) and testing (67 studies) sets (Table 2).

Training set sensitivity for localization of fractures within each vertebra was 0.82 relative to the reference standard (28 of 34; 95% confidence interval [CI]: 0.68, 0.90) at an FPR of 2.5 per patient (Table 3). Training set sensitivity for fracture localization on the correct vertebral level (T1–L5) was 0.88 (23 of 26; 95% CI: 0.72, 0.96) at an FPR of 1.3 per patient. Testing set sensitivity for localization of fractures within each vertebra was 0.81 (87 of 107; 95% CI: 0.75, 0.87) with an FPR of 2.7. Test set sensitivity for fracture localization on the correct vertebral level was 0.92 (55 of 60; 95% CI: 0.79, 0.94) with an FPR of 1.6. FROC curves are shown in Figure 3. The testing and training sets did not demonstrate a statistically significant difference in sensitivity, with a bivariate χ^2 test statistic of 0.074 (P = .79).

Test set sensitivity for male patients was 0.82 (62 of 76) with an FPR of 2.8 and that for female patients was 0.81 (25 of 31) with an FPR of 2.1. Results of the t test showed that there was not a statistically significant difference between male and female cohorts (P = .99 for sensitivity and P = .25 for FPR).

Examples of TP, FP, and false-negative detections are illustrated in

Figure 3

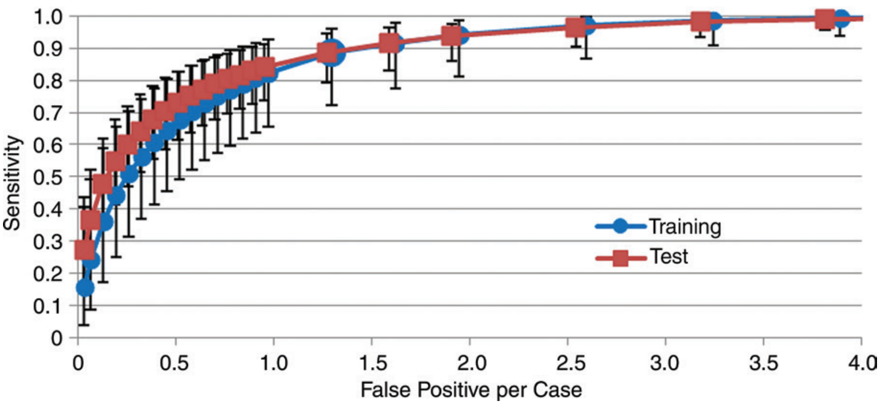

Figure 3: Graph demonstrates FROC analysis of computer localization of fractured vertebral bodies. The training set FROC curve of SVM performance for localization of fractures within each vertebra demonstrates 88% sensitivity (95% CI: 72%, 96%) at an FPR of 1.3 lesions per patient. The testing set FROC curve of SVM performance demonstrates 92% sensitivity (95% CI: 79%, 94%) at an FPR of 1.6 lesions per patient.

Figure 4

Figure 4: Axial CT section demonstrates a TP detection in a 52-year-old man with a Denis two-column fracture of an L4 vertebral body. Fracture of the posterior spinous process is also noted; however, this region is not yet included in the fracture search area of the algorithm. Thus, this is an overall Denis three-column fracture of the vertebral body and posterior elements. The computer algorithm marked the automated detection in green on the image.

Figures 4–8. Additional examples of each type of detection are found in Figures E2–E6 (online). There were 272 FP findings, with 106 (39%) due to nutrient foramina, 54 (20%) due to costovertebral junctions, 52 (19%) due to degenerative osteophytes, 38 (14%) due to intervertebral disk spaces, and three (1%) due to other causes. Nineteen (7%) of initially marked FP detections were found to be true detections on review, overlooked on creation of the reference data set. There were 26 false-negative findings, with 14 of 26 (54%) due to fracture lines paralleling and in close proximity to a vertebral body end plate, three of 26 (12%) due to degenerative joint disease, three due to FP manual interpretation in the reference testing set seen as negative at retrospective repeat review, two due to proximity and extension into foramen, two due to proximity to the costovertebral junction, one due to low spatial resolution owing to a large field of view, and one due to proximity to adjacent vertebral burst fracture.

The Denis column classification of fracture pattern involvement (anterior, middle, or anterior and middle) was determined by our system and validated against radiologist assessment. Examples of column classifications by the radiologist and the computer system are shown in Figure 9 and Figures E7–E9 (online). The confusion matrix is shown in Table 4. The system correctly classified Denis column involvement in 68 of 86 (79%) of the fractured vertebrae. The calculated κ coefficient was 0.574 (95% CI: 0.399, 0.749), consistent with moderate agreement.

Discussion

We have developed and validated a computer system to detect traumatic vertebral body fractures, provide the appropriate enumerated level of the injured vertebra, and spatially localize the fracture within the injured vertebra. A sample classification task involving quantitative features was performed.

Fractures through vertebrae have numerous potential trajectories and comminution patterns. In the development of the theoretical model that forms the functional basis of this algorithm, we hypothesized that a simple fracture (a surface or two-manifold fracture in three-dimensional space) that transects a cylinder of brittle material subjected to high-energy trauma should almost necessarily involve the side of the cylinder, regardless of fracture geometry. Taking the vertebral body in the first approximation as an essential rigid cylinder thus creates a unifying model to detect most fracture types by means of examination of the anterior, posterior, and lateral cortex, the central element of this fracture detection algorithm. Additional motivation for this framework lies in the increased fracture conspicuity in the relatively homogeneous vertebral cortex compared with typical semiuniform heterogeneity of marrow space, presumptively increasing the sensitivity for fracture detection. Finally, by separating the cortex from the underlying medullary space and mapping the cortex into a plane, a three-dimensional detection problem is converted into a simpler two-dimensional problem. This two-dimensional surface is then remapped onto the vertebra for three-dimensional fracture localization.

The system has potential for application to osteoporotic compression fracture cases in detecting vertebral body wall cortical breaks. However, owing to the altered material characteristics of the osteopenic bone, there

Figure 5

Figure 5: Axial CT section demonstrates a TP detection in a 32-year-old man with a Denis two-column fracture involving the left-sided superior end plate of an L1 vertebral body. The computer algorithm marked the automated detection in green on the image.

Figure 6

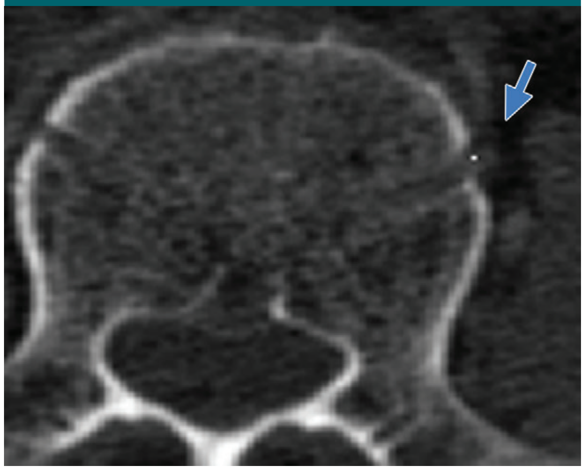

Figure 6: Axial CT section demonstrates an FP detection in a 57-year-old man with nutrient foramen of the L2 vertebra. The computer algorithm marked the automated detection with a white pixel. An arrow has been placed for clarification.

Figure 7

Figure 7: Axial CT section demonstrates an FP detection in a 62-year-old woman with costovertebral junction of the T10 vertebra. The computer algorithm marked the automated detection with a white pixel. An arrow has been placed for clarification.

Figure 8

Figure 8: Axial CT section demonstrates a false-negative detection in a 14-year-old adolescent girl with a nondisplaced, transversely oriented fracture of the T5 vertebra. The point of cortical extension of the fracture near the costovertebral junction has been marked with a red pixel. An arrow has been placed for clarification.

Figure 9

Figure 9: Axial CT section in a 22-year-old man demonstrates a Denis column classification of fracture involvement. In this misclassification example, the radiologist classification was anterior and middle column involvement, and computer system classification was isolated anterior column fractures in the L5 vertebra. The arrow denotes the left lateral wall extension of the fracture.

is potential for oversight of isolated end plate fractures not in the design parameters of this system.

The system performed with 92% sensitivity for fracture detection and localization on the correct vertebral level, with improvement anticipated in future versions. Sensitivity variation between testing and training sets was not statistically significant, suggesting data set independence and generalizability.

Our system generates quantitative fracture pattern data for injury classification and has the potential

Table 4

Denis Column Classification of Fracture Pattern

Computer Classification	Classified as Anterior by the Radiologist	Classified as Middle by the Radiologist	Classified as Anterior and Middle by the Radiologist
Anterior	20	0	14
Middle	1	2	0
Anterior and middle	3	0	46

Note.—Data are the number of fractures.

to decrease interobserver variability of fracture classification. The speed of algorithm analysis and detailed quantitative anatomic information extracted from each injury site portend a future ability to provide timely, repeatable, and detailed assessment of spine fracture patterns to fit the varied schema of multiple evolving trauma surgery classification systems. Quantitative features generated may also aid in comparative effectiveness research needed to guide the development of new clinical treatment paradigms based on patient outcomes and evidence-based medicine studies (34).

We used three-dimensional quantitative features to localize regions of fracture involvement within each vertebra. Isolated Denis anterior column fractures (eg, compression-type fractures) are differentiated from combined anterior and middle column fractures (burst type) by the system. Motivation for this task arises from the three-column description of Denis, in which spinal instability is determined when any two of the three Denis spinal columns are disrupted (18,19). Additional motivation for this sample task arises from clinical practice, where the Denis three-column model is the most commonly used classification system (35). The Denis classification system has been previously reported to demonstrate fair to good interobserver reliability (36). Denis column classification agreement of 79% was obtained by the computer system relative to radiologist classification, with a κ score consistent with moderate agreement. Confusion matrix analysis suggests that the predominant factor lowering the κ score is fracture locus classification as anterior column by the system and combined anterior and middle column by the radiologist. This variant classification may arise from subjective localization of Denis column boundaries by the radiologist during the qualitative visual review process, particularly in cases with fractures that terminate near the column boundaries, compared with the quantitative and explicit column division by the system (see the limitations paragraph). Another possible cause of these variant classifications may be fracture proximity to the vertebral end plate, as the algorithm detects and segments the sides of the vertebral body but not the end plate. The sides of the vertebral body smoothly curve into the end plate; thus, the algorithm likely loses some accuracy near this transition.

Although the software application was tested for Denis column classification, there are numerous classification systems in clinical use with substantial variability in relevant imaging features. For example, the Thoracolumbar Injury Classification and Severity Score system imaging features include vertebral height loss, translation, and canal diameter (37). The McCormack Load Sharing classification is used to assess sagittal plane deformity, fracture fragment distraction, and extent of vertebral body involvement (6). We plan to integrate our previously validated software for vertebral body height loss into the next phase of system development (23), thus combining direct detection and characterization of fracture lines with detection and measurement of global geometric deformity. This multiscale ability to detect and classify fracture patterns by means of quantitative image analysis will allow simultaneous class assignment in multiple classification systems now in use, allowing the interpreting radiologist to provide timely assignment to any of a number of classification schema preferred by the treating trauma surgeon at the time of injury.

There were several limitations in the fracture detection system design. First, the fracture search was limited to the bodies of the vertebrae. This approach was chosen to simplify a large complex problem by division into smaller, more manageable, modular pieces, with algorithmic design to detect fractures of the geometrically simpler vertebral bodies, thereby reducing algorithm complexity. Clinical utility was also considered in this design phase. In the Denis three-column model of the spine, injury of the posterior aspect of the vertebral body (the Denis "middle column") is an essential element in the determination of spinal instability. Thus, limitation of the fracture search region to the vertebral body may maintain clinical relevance by means of detection of middle column fractures (5). Second, the algorithm created and tested in our study is specific for detection of fracture discontinuities on vertebral body cortices. This anatomic simplification was believed to be justified on the basis of the assumption that this work is intended to demonstrate the unifying characteristic shared by essentially all vertebral body fracture geometries—involvement of the sides of the vertebral body. An exception would include focal vertebral body end plate fractures without sidewall involvement, as in an end plate–only fracture, a presumed unusual occurrence in patients with nonosteopenic trauma. Third, the FPR is relatively high. Two of the three most common causes (nutrient foramen and costovertebral junctions) may be decreased by a more sophisticated segmentation algorithm design, and the third (irregular end plate osteophytes) may be decreased by the addition of an algorithm, now in development, to detect degenerative change of the vertebrae. Elimination of these three causes of FP findings would eliminate 78% of FP detections. Fourth, image assessment by the radiologist on the picture archiving and communication system for Denis column classification of the fractures was performed to emulate the typical method of clinical practice study review, without column boundaries electronically delineated on the images. The qualitative nature, fine-scale variability, and subjectivity of this manual classification process may have resulted in misclassification of fractures that terminated near the column boundary, and system performance relative to absolute quantitative standards may be somewhat higher than reported here. Fifth, images were reconstructed with a soft-tissue kernel to decrease image noise effects on software performance.

In conclusion, we designed and validated a fully automated quantitative image analysis system that can directly detect fractures of the anterior, posterior, and lateral cortex of thoracic and lumbar vertebral bodies on CT images, discern the level of fractured vertebrae, and localize fractures within the vertebral body.

Acknowledgment: We thank Andrew Dwyer, MD, of the National Institutes of Health Clinical Center, for critical manuscript review.

Disclosures of Conflicts of Interest: **J.E.B.** disclosed no relevant relationships. **J.Y.** disclosed no relevant relationships. **H.M.** disclosed no relevant relationships. **R.M.S.** Activities related to the present article: disclosed no relevant relationships. Activities not related to the present article: institution received grants from iCAD Medical for research support; author received money from Johnson & Johnson as a former stockholder; institution received grants from Viatronix in the form of providing free software to the author's laboratory; author and institution received patent royalties from iCAD Medical. Other relationships: disclosed no relevant relationships.

References

1. Saylor PJ, Smith MR. Bone health and prostate cancer. Prostate Cancer Prostatic Dis 2010;13(1):20–27.
2. Anderson S, Biros MH, Reardon RF. Delayed diagnosis of thoracolumbar fractures in multiple-trauma patients. Acad Emerg Med 1996;3(9):832–839.
3. Parizel PM, van der Zijden T, Gaudino S, et al. Trauma of the spine and spinal cord: imaging strategies. Eur Spine J 2010;19(Suppl 1):S8–S17.
4. Joaquim AF, Patel AA. Thoracolumbar spine trauma: evaluation and surgical decision-making. J Craniovertebr Junction Spine 2013;4(1):3–9.
5. Kepler CK, Felte RF, Rihn JA. Current concepts: classification of thoracolumbar fractures. Semin Spine Surg 2012;24(4):210–215.
6. Sethi MK, Schoenfeld AJ, Bono CM, Harris MB. The evolution of thoracolumbar injury classification systems. Spine J 2009;9(9):780–788.
7. Denis F. The three column spine and its significance in the classification of acute thoracolumbar spinal injuries. Spine 1983;8(8):817–831.
8. McAfee PC, Yuan HA, Fredrickson BE, Lubicky JP. The value of computed tomography in thoracolumbar fractures. An analysis of one hundred consecutive cases and a new classification. J Bone Joint Surg Am 1983;65(4):461–473.
9. Magerl F, Aebi M, Gertzbein SD, Harms J, Nazarian S. A comprehensive classification of thoracic and lumbar injuries. Eur Spine J 1994;3(4):184–201.
10. McCormack T, Karaikovic E, Gaines RW. The load sharing classification of spine fractures. Spine 1994;19(15):1741–1744.
11. Vaccaro AR, Lehman RA Jr, Hurlbert RJ, et al. A new classification of thoracolumbar injuries: the importance of injury morphology, the integrity of the posterior ligamentous complex, and neurologic status. Spine 2005;30(20):2325–2333.
12. Joaquim AF, Patel AA. Relationships between the Arbeitsgemeinschaft für Osteosynthesefragen Spine System and the Thoracolumbar Injury Classification System: an analysis of the literature. J Spinal Cord Med 2013;36(6):586–590.
13. Parker JW, Lane JR, Karaikovic EE, Gaines RW. Successful short-segment instrumentation and fusion for thoracolumbar spine fractures: a consecutive 4½-year series. Spine 2000;25(9):1157–1170.
14. Vaccaro AR, Lim MR, Hurlbert RJ, et al. Surgical decision making for unstable thoracolumbar spine injuries: results of a consensus panel review by the Spine Trauma Study Group. J Spinal Disord Tech 2006;19(1):1–10.
15. Sansur CA, Shaffrey CI. Diagnosis and management of low lumbar burst fractures. Semin Spine Surg 2010;22(1):33–37.
16. Mirvis SE. Increasing workloads in radiology: does it matter? Appl Radiol 2013;42:6–7.
17. Krupinski EA, Berbaum KS, Caldwell RT, Schartz KM, Kim J. Long radiology workdays reduce detection and accommodation accuracy. J Am Coll Radiol 2010;7(9):698–704.
18. Patel AA, Vaccaro AR. Thoracolumbar spine trauma classification. J Am Acad Orthop Surg 2010;18(2):63–71.
19. Kim CW, Perry A, Garfin SR. Spinal instability: the orthopedic approach. Semin Musculoskelet Radiol 2005;9(1):77–87.
20. Guglielmi G, Diacinti D, van Kuijk C, et al. Vertebral morphometry: current methods and recent advances. Eur Radiol 2008;18(7):1484–1496.
21. Guglielmi G, Palmieri F, Placentino MG, D'Errico F, Stoppino LP. Assessment of osteoporotic vertebral fractures using specialized workflow software for 6-point morphometry. Eur J Radiol 2009;70(1):142–148.
22. Ghosh S, Alomari RS, Chaudhary V, Dhillon G. Automatic lumbar vertebra segmentation from clinical CT for wedge compression fracture diagnosis. In: Summers RM, van Ginneken B, eds. Proceedings of SPIE: medical imaging 2011—computer-aided diagnosis. Vol 7963. Bellingham, Wash: International Society for Optics and Photonics, 2011; 796303.
23. Yao J, Burns JE, Wiese T, Summers RM. Quantitative vertebral compression fracture evaluation using a height compass. In: van Ginneken B, Novak CL, eds. Proceedings of SPIE: medical imaging 2012—computer-aided diagnosis. Vol 8315. Bellingham, Wash: International Society for Optics and Photonics, 2011; 83151X.
24. Hsieh MS, Tsai MD, Yeh YD, Jou SB. Automatic spinal fracture diagnosis and surgical management based on 3D image analysis and reconstruction of CT transverse sections. Biomed Eng Appl Basis Commun 2002;14(5):204–214.
25. Yao J, Burns JE, Munoz H, Summers RM. Detection of vertebral body fractures based on cortical shell unwrapping. Med Image Comput Comput Assist Interv 2012;15(Pt 3):509–516.
26. Aebi M. Classification of thoracolumbar fractures and dislocations. Eur Spine J 2010;19(Suppl 1):S2–S7.
27. Bernstein M. Easily missed thoracolumbar spine fractures. Eur J Radiol 2010;74(1):6–15.
28. Yao J, O'Connor SD, Summers RM. Automated spinal column extraction and partitioning. In:Biomedical Imaging: Nano to Macro, 2006. 3rd IEEE International Symposium on: IEEE, 2006; 390–393.

29. Pontil M, Verri A. Support vector machines for 3D object recognition. IEEE Trans Pattern Anal Mach Intell 1998;20(6):637–646.

30. Burges CJ. A tutorial on support vector machines for pattern recognition. Data Min Knowl Discov 1998;2(6):121–167.

31. Osher S, Sethian JA. Fronts propagating with curvature-dependent speed: algorithms based on Hamilton-Jacobi formulations. J Comput Phys 1988;79(1):12–49.

32. Yao J, O'Connor S, Summers R. Computer aided detection of lytic bone metastases in the spine using routine CT images. In: Biomedical Imaging: From Nano to Macro, 2007. ISBI 2007. 4th IEEE International Symposium on. Arlington, VA: IEEE, 2007; 512–515.

33. Yao J, Summers RM, Hara AK. Optimizing the support vector machines (SVM) committee configuration in a colonic polyp CAD system. In: Amir AA, Manduca A, eds. Proceedings of SPIE: medical imaging 2015: physiology, function, and structure from medical images. Vol 5746. Bellingham, Wash: International Society for Optics and Photonics, 2005; 384–392.

34. Gazelle GS, Kessler L, Lee DW, et al. A framework for assessing the value of diagnostic imaging in the era of comparative effectiveness research. Radiology 2011;261(3):692–698.

35. Lewkonia P, Paolucci EO, Thomas K. Reliability of the thoracolumbar injury classification and severity score and comparison with the Denis classification for injury to the thoracic and lumbar spine. Spine 2012;37(26): 2161–2167.

36. Oner FC, Ramos LM, Simmermacher RK, et al. Classification of thoracic and lumbar spine fractures: problems of reproducibility. A study of 53 patients using CT and MRI. Eur Spine J 2002;11(3):235–245.

37. Rihn JA, Anderson DT, Harris E, et al. A review of the TLICS system: a novel, user-friendly thoracolumbar trauma classification system. Acta Orthop 2008;79(4):461–466.